SAND2009-5673C

An Optical Study of Mixture Preparation in a Hydrogen-fueled Engine with Direct Injection Using Different Nozzle Designs

Victor M. Salazar, Sebastian A. Kaiser
Sandia National Laboratories

ABSTRACT

Mixture formation in an optically accessible hydrogen-fueled engine was investigated using Planar Laser-Induced Fluorescence (PLIF) of acetone as a fuel tracer. The engine was motored and fueled by direct high-pressure injection. This paper presents the evolution of the spatial distribution of the ensemble-mean equivalence ratio for six different combinations of nozzle design and injector geometry, each for three different injection timings after intake-valve closure. Asymmetric single-hole and 5-hole nozzles as well as symmetric 6-hole and 13-hole nozzles were used. For early injection, the low in-cylinder pressure and density allow the jet to preserve its momentum long enough to undergo extensive jet-wall and (for multi-hole nozzles) jet-jet interaction, but the final mixture is fairly homogeneous. Intermediately timed injection yields inhomogeneous mixtures with surprisingly similar features observed for all multi-hole injectors. Fuel is concentrated near the cylinder wall, an unfavorable scenario were the engine to be fired. Results for late injection depend more on the particular injector configuration. The 13-hole injector shows complete merging of all jets, consistent with results in the literature. The influence of intake-induced bulk-gas tumble is minor for the current injector and combustion-chamber configurations.

INTRODUCTION

Hydrogen-fueled internal combustion engines (H2ICEs) can be highly efficient power plants in vehicles, meeting present and future emissions regulations at reasonable cost [1, 2]. A key element of advanced H2ICEs is direct injection (DI) of the hydrogen fuel into the cylinder [3, 4]. With DI it is possible to mitigate pre-ignition and backfire, increase power density, and recover part of the energy stored in the form of high fuel pressures. Most importantly, the engine developer can devise injection strategies to improve the trade-off between efficiency and NOx. However, this requires knowledge about the injection event, in-cylinder mixing, and the resulting pre-combustion mixture distribution. Much can be learned from careful parametric studies on single-cylinder research engines [5]. Ideally, these metal-engine studies are complemented by laser-based measurements in optically accessible engines and numerical simulations to gain physical insight into these processes. As in optical gasoline and diesel engines, Planar Laser-Induced Fluorescence (PLIF) of a fuel-tracer can be used in DI-H2ICEs to make two-dimensional measurements of the instantaneous fuel distribution.

Using optical diagnostics in a fully optically accessible engine, we aim to provide some physical understanding of the in-cylinder processes that will be necessary to design future DI-H2ICEs. Previous studies on this engine, albeit at operating points different from the ones studied here, included OH* chemiluminescence imaging [6] and measurements of velocity and fuel distribution [7, 8]. The aim of the current study is to investigate in detail the influence of injector location and geometry and injection timing on mixture preparation. To this end, the equivalence ratio was measured in the motored engine in several horizontal planes for a series of crank angles, up to the MBT spark timing from a very similar all-metal engine at Argonne National Laboratory [5, 9]. The high quality of the PLIF data can be used to evaluate several aspects of in-cylinder air/fuel mixing, but for brevity we will here restrict the analysis to a description of the evolution of the ensemble-mean fuel distribution.

Bore	92 mm
Stroke	85 mm
Displacement	560 cm^3
Compression ratio	11
Speed	1500 rev/min
Intake pressure	1 bar
Fired IMEP	2.5 bar
Global equiv. ratio	≈ 0.25
Injection pressure	80 - 116 bar (depending on injector)
Injection duration	18.5 – 22 °CA (depending on injector)
Intake valve timing[1]	IVO: 346° CA / IVC: -140° CA
Exhaust valve timing	EVO: 130° CA / EVC: -356° CA

Table 1: Specifications of engine and operating point.

EXPERIMENT

OPTICAL ENGINE AND INJECTION CONFIGURATION

The engine under consideration is a passenger-car sized single-cylinder research engine with optical access of the Bowditch type, *i.e.*, through parts of the liner and pent-roof as well as through the flat-topped piston. Hydrogen fuel is delivered directly into the cylinder through an injector developed by Westport Inc. For all experiments here, the engine was motored and supplied with nitrogen in the intake. Table 1 summarizes essential engine and testing parameters and Figure 1 shows the general upper engine geometry. The intake system is omitted for clarity. It consists of two separate intake ports, one for each intake valve, both straight and parallel to each other. The ports form an angle of 45° with respect to the fire deck. The design serves to create tumble motion without any swirl in the combustion chamber. The engine head is a single-cylinder GM research head, which had previously been used for gasoline-fueled operation. It has not been modified or optimized for hydrogen fueling in any flow-relevant parts

Six combinations of injector-tip designs, injector locations, and jet targeting were investigated. They are (except for the 13-hole nozzle, see below) part of the same set of configurations used in previous performance studies [5, 9]. The different nozzle designs are shown in Figure 2a and are briefly described below.

- A single-hole nozzle with a 1.46 mm diameter hole at an angle of 50° with respect to the injector axis.
- A 6-hole nozzle with symmetric hole placement, a hole diameter of 0.54 mm, and an included cone angle of 90º.
- A 5-hole nozzle with asymmetric hole placement on one side of the transverse axis, a hole diameter of 0.61 mm, and a cone angle of the outer 4 holes of 70º.
- A 13-hole nozzle with 12 holes distributed symmetrically in two concentric circles with six holes each one plus the one at the center. The hole diameter was 0.38 mm, and the cone angle of all off-axis holes was 60°.

Multiple configurations were possible with respect to injector location and jet orientation. The following six configurations were used for this study:

- The single-hole injector in central location with the jet pointing along the top edge of the pent roof (1-hole central) as shown in Figure 3.
- The 6-hole injector in side location (6-hole side)
- The 6-hole injector in central location (6-hole central)
- The 5-hole injector in side location with the holes pointing upwards, along the pent roof (5-hole up)
- The 5-hole injector in side location with the holes pointing towards the piston top (5-hole down)
- The 13-hole injector in central location (13-hole central)

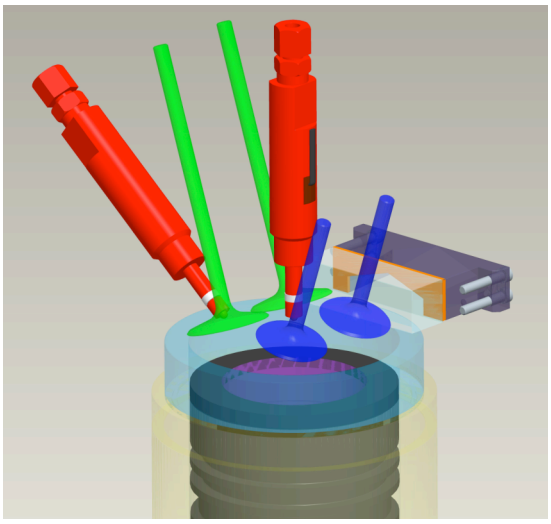

Figure 1: Selected parts of the head assembly. The injector is shown in both side and central location.

In the side location, the injector was oriented tilted 40° with respect to the fire deck, as shown schematically in Figure 2b. When mounted in the central location, the injector replaces the spark plug via a custom adapter

[1] The crank angle convention is -360° CA to 360° CA, with 0° CA corresponding to top dead center of the compression stroke.

sleeve. The orientation is vertical, *i.e.*, parallel to the cylinder axis. Because the spark plug is not in place when central injection is used, fired engine operation (for performance testing) is not possible for this configuration. The jet orientation for the single-hole injector is shown in Figure 3, and in the same schematic the relative size of the field of view with respect to the cylinder diameter is shown.

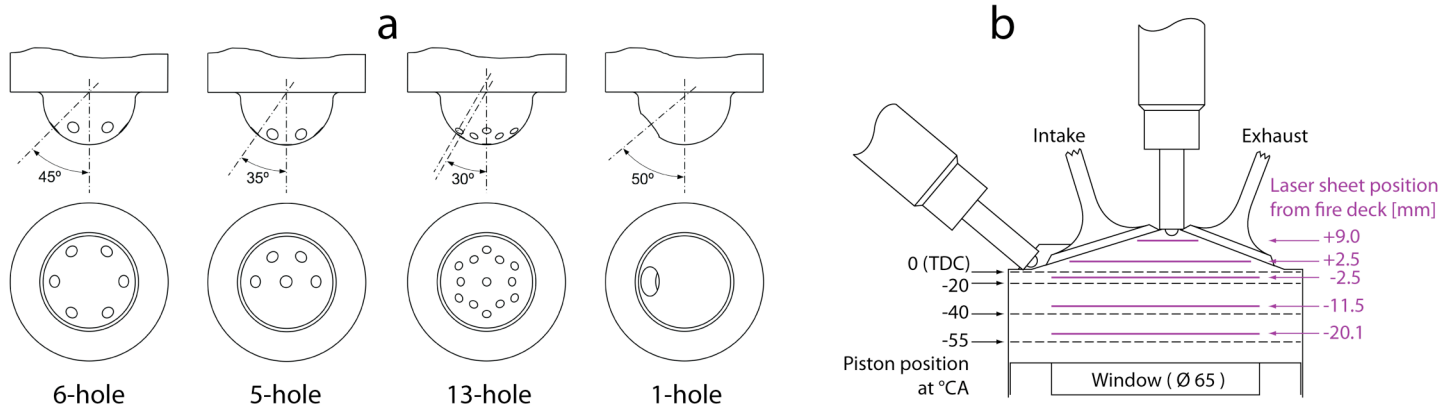

Figure 2: (a) Injector tip designs. (b) Schematic of the combustion chamber with positions of measurement planes and piston at a few crank angles.

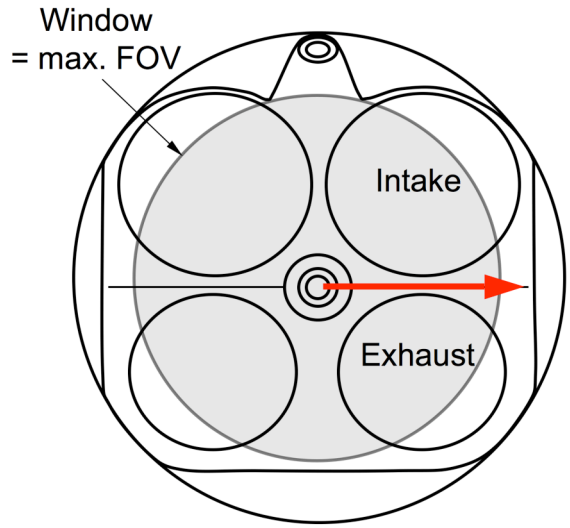

Figure 3: Schematic of the cylinder head showing field of view (shaded area) and the jet direction for the single-hole injector (red arrow).

DIAGNOSTIC TECHNIQUE

The PLIF imaging technique used to measure the in-cylinder fuel distribution is described in detail in reference 10. Briefly, acetone is seeded as a tracer into the hydrogen fuel by a high-pressure bubbler. At 100 bar and room temperature, a volume concentration of 0.33% can be reached. A quadrupled Nd:YAG at 266 nm laser excites fluorescence in a plane parallel to the piston. Laser energies of about 100 mJ/pulse and a sheet-forming lens combination with f = 1500 mm were used. An f = 85 mm, *f*/1.4 camera lens focuses the visible part of the resulting acetone fluorescence onto an unintensified, back-illuminated CCD. Standard background and flat-field corrections are performed to quantify the measurements. For the latter, a nearly homogeneous charge is prepared by DI during the intake stroke. Inhomogeneities in the temperature field, induced by mixing of cold hydrogen and hot bulk gas, are corrected for based on known spectroscopic properties of the tracer [11, 12] and the assumption of adiabatic mixing between fuel and bulk gas [10, 13, 14, 15]. The overall typical maximum error in the ensemble-mean equivalence-ratio fields is estimated to be 25%.

EXPERIMENTAL CONDITIONS

In this study, we concentrated on pre-combustion fuel/bulk-gas mixing. In a combusting mixture, PLIF measurements after start of combustion are possible and can deliver interesting qualitative information [for example, see reference 16]. However, after spark, quantification of the signal becomes very challenging. An estimate of the applicable spark timing for each configuration was obtained as the maximum brake torque (MBT) spark timing in a very similar all-metal DI-H2ICE at Argonne National Labs [5, 9], and is referred to in this paper as “spark”, “ignition”, etc. These experiments also gave an indication as to what injection timings would yield practically useful, stable engine operation. Except for the injection pressure, that engine was operated under identical conditions (i.e., those of Table 1) as the optical engine. The injection pressure in the optical engine had to be adjusted somewhat to yield the same equivalence ratio and injection duration as in the metal engine. The overall equivalence ratio was calculated from steady-state nitrogen and hydrogen flow rates, taking nitrogen to be a substitute for air (21% O_2 / 79% N_2).

For each injector configuration, three different injection timings (as given by the start of injection, SOI) were investigated:

- -140°CA, the earliest possible SOI after intake valve closure (IVC)
- -80°CA, the latest timing for which the fired metal engine operated stably *for all six* injector configurations
- -40°CA, the latest timing for which the metal engine operated stably for *at least two injector* configurations (6-hole side, 1-hole central)

Measurements were made for several crank angles ranging from midway through the injection (SOI + 10°CA) to the presumed spark timing. Depending on the crank angle at the time of imaging, PLIF data were taken in up to 5 planes spaced throughout the upper part of the cylinder and pent-roof, as shown in Figure 2b. The central 65 mm of the 92 mm bore were visible through the piston window. Images from 135 fueled cycles were acquired per measurement plane.

RESULTS AND DISCUSSION

In this section the evolution of the mixing process is studied. Several injection configurations (from single-hole to multi-hole injectors) are analyzed. The section closes with a comparative analysis of the fuel distribution at "ignition" for the intermediate injection timing.

1-HOLE CENTRAL

The single-hole injector was studied to gain physical insight into the mixture formation process while avoiding the complexities of jet-to-jet interactions and multiple jet-wall interactions associated with a multi-hole nozzle. An additional benefit of this configuration is the flexibility to point the jet at any polar angle; however, for the present study the jet direction was kept at the fixed position indicated in Figure 3. This particular orientation was chosen based on the performance testing reported in reference 9, which showed that this direction provided the best performance and the widest range of stable operation. Other orientations may be evaluated optically in the future.

The images of the ensemble-mean equivalence-ratio in Figure 4 show the evolution of the fuel distribution for different injection timings. For image timings later than -70°CA the piston top is drawn schematically to indicate the lower boundary of the combustion chamber at each time. This is also to remind the reader visually that a significant portion of the cylinder volume –the near-wall regions and everything more than 20 mm below the fire deck– cannot be imaged and is not shown. The first image set in each time series essentially shows where the injector's jet is aimed. The lag between injection command and start of needle lift is about 3°CA or 0.33 ms at 1500 rev/min, hence the first image set is taken 7°CA after the jet start.

For early injection (SOI = -140°CA), Figure 4 shows that within these 7°CA, corresponding to 1.1 ms at 1500 rev/min, the jet has penetrated through the optically accessible region of the cylinder. Due to the horizontally and vertically restricted field of view, it is not clear if the jet has impinged on the cylinder wall. At -100°CA the injection process has ended (the injection duration is 18.5°CA), and the top planes are devoid of fuel except at their borders where fuel coming from jet-cylinder wall interaction is seen. It is remarkable how little fuel remains near the injector after the injection event is over. This "leaning" of the near-nozzle region is quite generic in transient jets, and it has also been observed in transient single-phase liquid jets [17] and the gas phase of diesel-like jets [18]. Musculus [19] uses a simple model to explain the associated enhanced entrainment of ambient bulk gas.

At -100°CA, the two bottom planes show a region of high fuel concentration near the cylinder wall opposite from where the jet is pointing, indicating that the impinged fuel has already "rolled over" the piston and cylinder walls. As the fuel cloud moves along the walls it entrains air and becomes leaner. The border between rich and lean sides fluid is well defined, not only in the ensemble mean of Figure 4, but also in single shots not shown here. This sharp boundary is characteristic of penetrating free and wall jets.

The roll-over of the fuel cloud continues throughout the remainder of the compression stroke such that at "spark" (*i.e.,* MBT spark timing from the metal engine) the highest concentration ends up again on the side where the fuel was injected. The jet convection slows down significantly late in the cycle. Between -130°CA and -70°CA the jet has penetrated to the piston top and then propagated along the opposite side, but between -70°CA and -20°CA the resulting fuel-rich cloud only shifts along the pent-roof by about half the piston diameter. This slowing of convection may be due to dissipation of the original jet momentum and enhanced entrainment at the higher pressure at later crank angles. Similar to the well-known late-cycle breakdown of intake tumble there could also be break-down of the large vortex induced by the injection into smaller ones. Direct velocity measurements, planned for future work, would help clarify the evolution of the jet-induced flow. The sharp gradient in the horizontal direction convects and dissipates to become a shallower vertical gradient at -40°CA, with a lean bottom plane near the piston top. However, by -20°CA the remaining weak gradients are mostly vertical again. Over the entire jet "round-trip" the fuel distribution becomes only slightly asymmetric in the transverse direction, indicating weak influence of the bulk gas's tumble motion, which would tend to push the fuel to one side.

When the fuel is injected at SOI = -80°CA (intermediate timing), the initial fuel distribution (at -70°CA) appears to show a reduction in the jet-spread angle. This is even more pronounced at SOI = -40°CA. However, Figure 4

displays the image series for all three injection timings on the same color scale. The width of a jet is measured based on self-similarity of the cross-section, in this case at an equivalence ratio that relative to the peak found in the respective jet cross-section. Enhanced entrainment, which would be expected from later injection with the accompanying higher in-cylinder pressure, reduces the peak equivalence ratio. Therefore, at identical color mapping, the jet may appear to have a smaller cross-section. Proper assessment of the spreading would need to scale for the mean peak equivalence-ratio in the cross-section. For vaporizing diesel jets [20] it has been found experimentally that, consistent with enhanced entrainment, the jet-spread angle increases with ambient pressure.

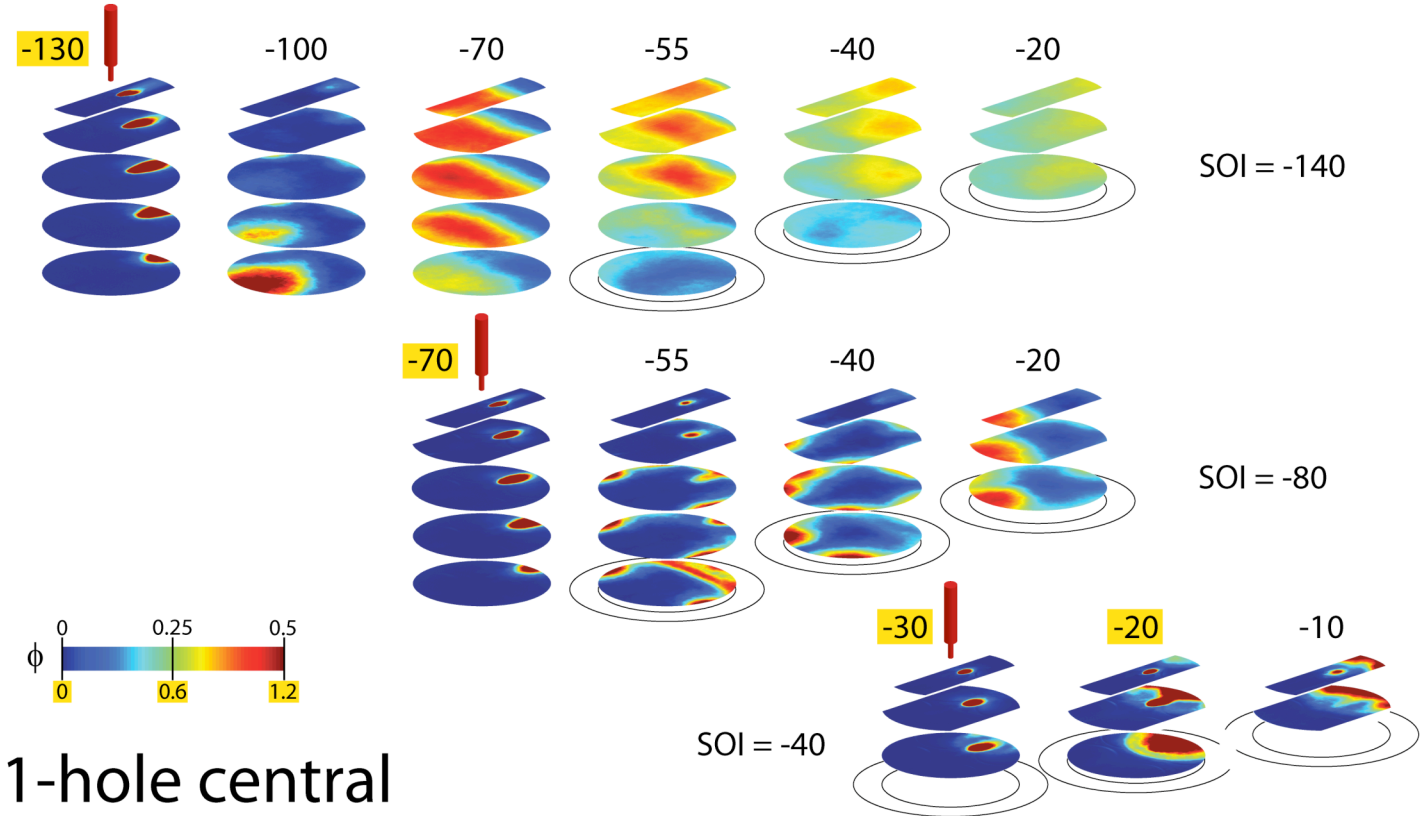

Figure 4: Time series of the mean equivalence ratio as measured by PLIF for three injection timings for the single-hole injector in central location. The vertical spacing between the images has been increased compared to the physical spacing of the planes to improve visual clarity. The color scale for the earliest imaging timings is different from that for the later ones, as indicated by the yellow highlighting

For SOI = -80°CA, the overall evolution of the jet into a fuel cloud deflected to make a round-trip (incomplete here) is similar to that of the early injection timing. At -55°CA the fuel injection has ended. Fuel impinging on the cylinder and piston walls can be seen in a pair of roll-up vortices near the cylinder walls. By -40°CA the impinged fuel has rolled over the piston surface and it is moving upwards along the cylinder walls. Due to the presence of the piston higher up in the cylinder and possibly also a larger spreading angle, this fuel has spread to be in the squish zone. This can clearly be seen comparing the images at -100°CA for early injection to those at -40°CA for intermediate injection, each image set being 40°CA after SOI. Later in the compression this fuel is pushed out to the very lean center of the combustion chamber. However, due to the reduced time and increased pressure, by -20°CA the fuel does not reach the spark plug region; consequently this injection strategy may not be optimal for stably-firing engine operation.

The images for SOI = -40°CA show that by -30°CA the fuel has penetrated the cylinder and impinged on the piston wall. Parts of the recirculation vortices from the jet impingement are seen near the jet core in the bottom plane, becoming more obvious for subsequent image timings. The fuel stays highly concentrated in the piston-cylinder corner. Regarding ignitability, at -10°CA the plane close to the spark shows a region rich in fuel, remaining from the jet wake due to the shorter time span available for post-injection entrainment. This may enable stably-firing operation of the engine.

As with early injection, also the intermediate and late injection cases show no evidence of the bulk-gas tumble motion disturbing the jet or its interaction with the walls. The fuel movement for this injector and experimental conditions are thus in general dominated by jet momentum redirected by fuel-wall interaction.

The key features of mixture formation with this particular single-hole configuration are as follows:

- Early injection initially yields little entrainment in the early stage of mixture formation, fast convection, and extensive jet-redirection such that a complete round-trip of the fuel cloud in a cross-tumble-like motion results. The time to “spark” is nevertheless sufficient for much homogenization.
- For intermediately timed injection the tumble-like fuel convection is modified by earlier interaction with the piston top, which spreads the fuel into the squish zones.
- Late injection yields drastically reduced fuel convection because of the shorter aspect ratio of the remaining cylinder volume, the increased in-cylinder pressure, and the reduction in available time. The fuel jet hits the piston top before the walls such that the circular motion seen for early injection does not occur.
- In general, towards the end of the compression stroke fuel convection slows significantly..
- Cross-flow from bulk-gas tumble has very little influence. This is probably due to the spatially concentrated input of momentum from the single-hole injector.

The study of the single-hole injector provided initial insight into the mixture formation, and this will help to understand the process in multi-hole injectors. In these injectors, momentum is not so spatially concentrated, but, in most designs, is dispersed over a range of different directions corresponding to the aiming of the various nozzles. This enhances entrainment, but means even more potential exists for jet-wall, jet-jet, and jet-bulk-flow interaction. Thus, to complement the single-hole injector study, the mixture-formation for different multi-hole injectors is investigated below.

6-HOLE SIDE

For the 6-hole injector in side location (Figure 5), the two top jets and the two side jets can be seen. The typical mushroom-like structure of the jet tip is visible in the top plane for SOI = -130°CA. At the low density early in the compression-part of the cycle the jets quickly penetrate and at -100°CA they have crossed the cylinder volume. A complex interaction of jet momentum, piston movement, and chamber walls ensues. At -100°CA the top jets have moved along the pent-roof such that the mixture in the top of the combustion chamber is very lean. In fact, the volume close to the injector has the lowest equivalence ratios of the entire imaged volume. This part of the cylinder is subsequently “filled back up” with hydrogen by the interaction of the side jets with cylinder liner and piston top. The process of fuel working its way back towards the injector takes the entire time to “spark”. At “spark timing” (-28°CA) the vicinity of the injector is still the leanest part of the combustion chamber. Surprisingly, there is no direct evidence of the presence of the two bottom jets. They are directed nearly vertically downward, and it seems that due to the long distance the jets can travel before they hit the piston top there is enough entrainment to achieve thorough dilution. Therefore, as the piston top pushes fluid upward, the region below the injector remains lean.

As expected from the single-hole results, jet penetration is much slower for later injection due to the higher bulk-gas density. For SOI = -80°CA this slower jet movement coupled with the shorter distance to the piston top and the shorter time to “spark” results in a poor fuel distribution. As a result, 40° after SOI (i.e., at -40°CA) much of the fuel is directly below the injector and to the sides, while after the same time span these regions were rather lean for SOI = -140°CA. At -26°CA the top jets have reached the squish volume opposite from the injector, and the piston has pushed up the fuel below the injector, so that a lean pocket in the center of the combustion chamber is surrounded by richer regions near the cylinder walls. For this injector configuration, the formation of a lean region in the center of the cylinder has also been observed for somewhat different operating conditions in previous work [8]. That investigation also included measurements of the flow field, which lead to the conclusion that jet-induced flow is re-directed by the walls to push lean bulk gas back towards the injector, inhibiting mixing for intermediate and late injection.

For the latest injection timing, SOI = -40°CA, observable jet-wall interactions are limited to fuel from the bottom two jets being pushed up by the piston. At -12°CA, measurements in the squish volume are not possible, but it can be presumed that the fuel distribution there resembles that at -20°CA, such that throughout the combustion chamber the highest equivalence ratios are found close to the injector.

6-HOLE CENTRAL

The configuration with central injection is particularly interesting due its symmetry. Again the difference in jet penetration between SOI = -140°CA and the later injection timings is very noticeable. Rapid leaning of the near-nozzle regions is also observed again. The important consequence of this latter feature is that for 6-hole central injection the space around where the spark plug would be (in a fired engine) is almost completely devoid of fuel after the injection. It does fill with more fuel-rich mixtures later in the cycle, but only after extensive jet-wall and jet-jet interaction. The latter causes the lower parts of the observable volume to have the highest equivalence ratios towards the center of the cylinder at -70°CA. The piston pushes up this central fuel cloud, but by -24°CA it is diluted too much to induce significant stratification. Also, for this early-injection case, enough jet momentum has dissipated such that the tumble motion remaining from the intake stroke introduces slight asymmetry in the fuel distribution, with lean regions away from the intake valves.

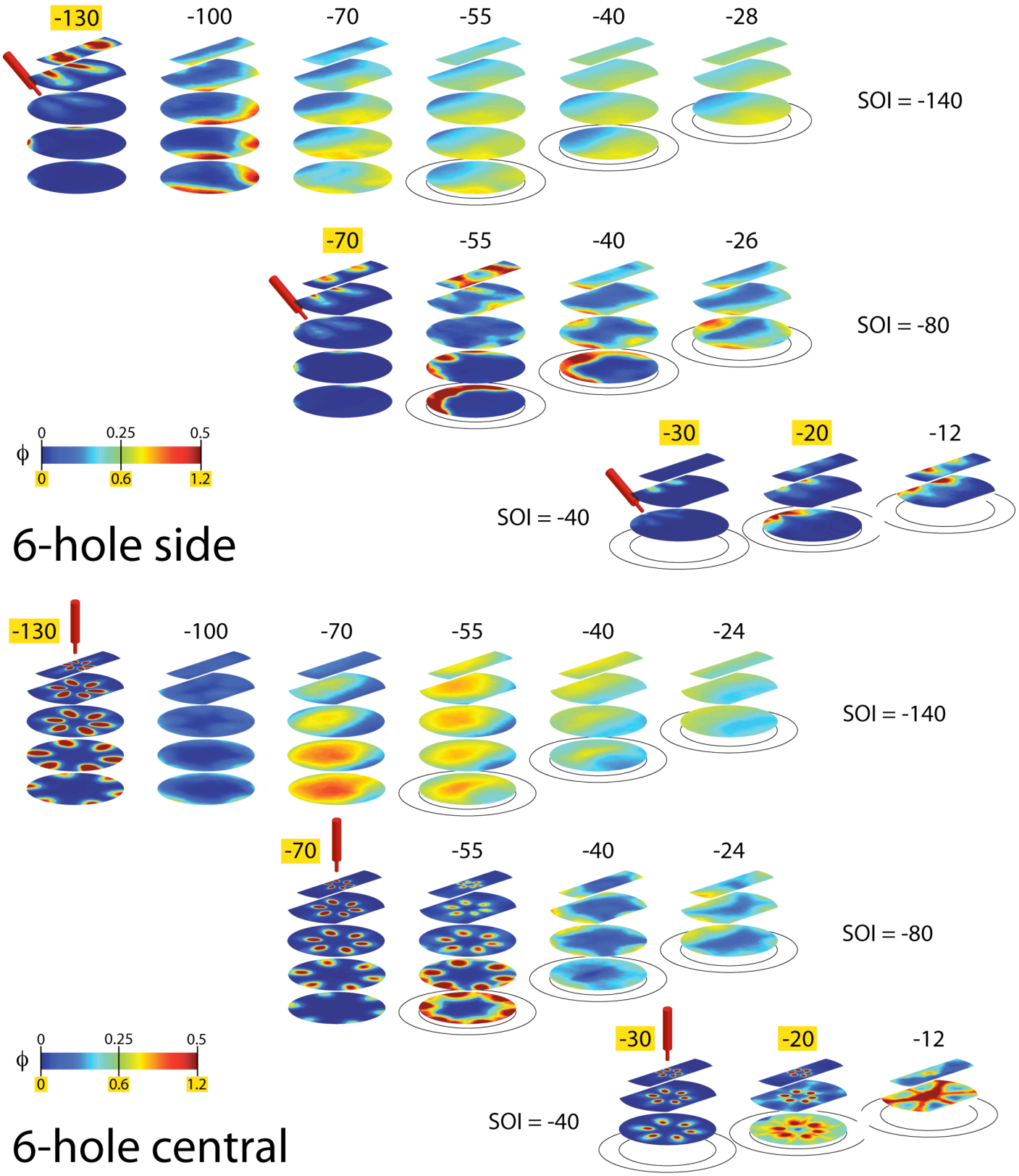

Figure 5: Same type of time series as in Figure 4. Top: 6-hole injector in side location. Bottom: 6-hole injector in central location.

For the two more retarded injection timings, a general observation is that, as in the case of retarded single-hole and 6-hole side injection, the fuel remains where it first interacts with a wall (piston, cylinder), because less time is available and the jet penetrates slower. The importance of jet-jet interactions on the mixture preparation can probably not be fully appreciated from ensemble-mean images, because they give only limited information about the intensity of local mixing. However, an interesting result of such interactions is the orientation of the star-shaped fuel-rich zone for SOI = -40°CA at -12°CA: The highest equivalence ratios are not found in the symmetry planes of the jets, but in between, where two adjacent jets have interacted after hitting the piston top.

From a practical point of view, for a simple single-injection strategy as examined here, this six-hole injector is ill-matched with a flat piston top. At -70°CA early injection (SOI = -140°CA) has actually produced a favorably stratified mixture, with fuel away from the wall and near the spark-plug location, but this occurs too early in the cycle. However, for intermediately-timed injection the earlier interaction with the piston top redirects the fuel into the squish volume, and for late injection the region near the spark plug is probably too lean for reliable fired operation. Although design optimization is outside of the scope of this paper, we may infer that a suitably shaped piston top could help create a more favorable fuel distribution.

5-HOLE UP

The general features and trends seen in the SOI-sweeps for the 6-hole injector are also found for this configuration: fast jet penetration and much jet-wall interaction for early injection, while later SOI results in slower penetration with the fuel remaining closer to the injector. For SOI = -140°CA (Figure 6) we can easily imagine the fuel-rich zone moving downwards and towards the cylinder wall opposite of the injector (-100°CA), then “bouncing” back while being pushed up by the piston (-70° to -26°CA). Tumble flow may help in making the regions far from the injector lean.

An interesting feature can be observed in the earliest image set for each SOI: The jets seem to emerge asymmetrically. Close inspection of the injector tip did not reveal any machining imprecision, which is not to say that the hardware is not possibly responsible for this behavior. Also the injector was carefully mounted such that the hole pattern was aligned with the symmetry planes of the cylinder as intended. An examination of single-cycle images (not shown) reveals that the asymmetries seen in the ensemble-mean are reflected in the instantaneous data, but also that there are large fluctuations. For example, the third plane from the top for SOI = -80°CA shows the (from point of the observer) left jet penetrating further, and the right jet having an irregular shape. However, in a significant number of shots the right jet penetrates further and appears more regularly shaped. Jet merging is observed as well, as in the experiments at TU Graz [16, 21]. The jet merging is influenced by large-scale turbulent fluctuations in the jets, resulting in cycle-to-cycle variations of the fuel distribution.

5-HOLE DOWN

Similarly to 6-hole central injection, much of the momentum in this configuration is directed downward. As a result the fuel distribution evolves similarly, at least for the two earlier injection timings (SOI = -140° and -80°CA), where jet-wall interaction is a dominant mechanism. In both cases a lean zone in the center is filled in from the sides. For SOI = -140° the filling-in process is slower with the 5-hole side configuration than it is with the 6-hole central injection. In the former, the lean region persists through the entire compression stroke, while in the latter the central region has become rich already by -70°CA. For SOI = -40°CA the higher spatial concentration of the momentum input by the 5-hole injector yields faster penetration for both 5-hole up and 5-hole down as compared to the 6-hole side configuration. Thus rich mixtures can be seen further away from the injector at -12°CA.

13-HOLE CENTRAL

Among the injectors investigated here, the 13-hole injector has the smallest included cone angle and by far the largest number of holes. Based on the results for the 5-hole injector, it was expected that due to the relatively small angle between contiguous jets some early jet-jet interaction could take place. Figure 7 shows equivalence-ratio maps for the three injection timings. For SOI = -140°CA individual jets cannot be identified clearly at -130°CA. The images show very little angular divergence between jets from different holes, indicating that all the jets have collapsed. The image closest to the injector tip reveals a star-shaped distribution reflecting the geometric pattern of the outer holes. This feature is observed in the successive planes as well, but as the jet moves downwards the feature vanishes and a unified rounded jet is observed.

The included cone angle of this injector is 60°. The vertical succession of jet cross-sections shows that the overall spread angle is much smaller, i.e. jet merging in the near field of the nozzle is taking place. This is consistent with high-speed Schlieren measurements by Petersen [22] in a constant-volume pressurized vessel. A sequence of measurements spanning the equivalent of about 8°CA is reproduced from that work in Figure 8. The injector was geometrically the same as the one used in the PLIF experiments, with comparable injection pressure and an ambient density typical of those found in engines. It can be seen that only in the region immediately below the injector tip single jets are present. Further downstream the jets merge and they appear as it they emerged from a single jet.

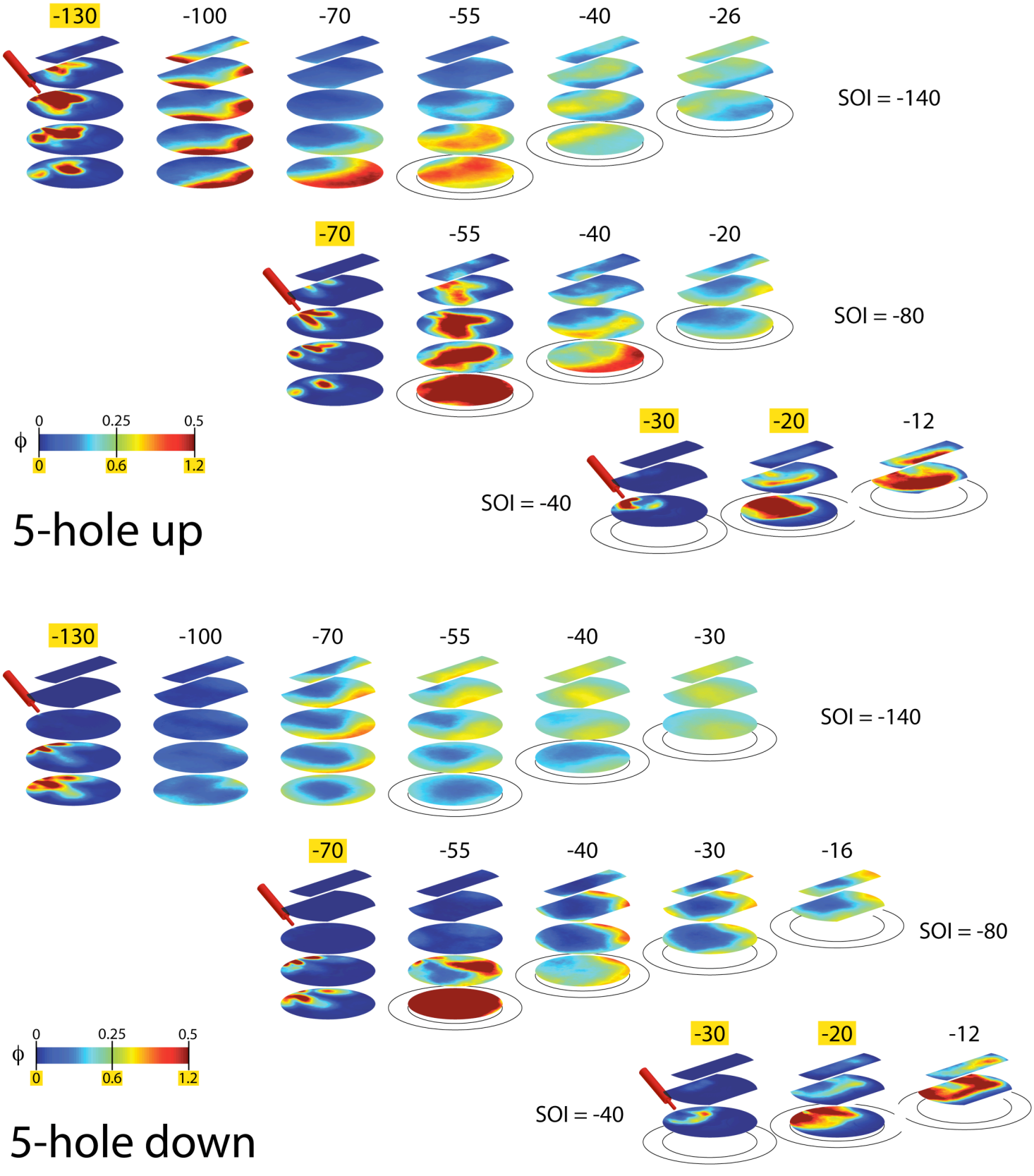

Figure 6: Same type of time series as in Figure 4. Top: 5-hole injector with hole pattern pointing upwards. Bottom: 5-hole injector with hole pattern pointing downwards.

Jet-jet merging reduces overall air entrainment. The greatest entrainment is obtained with the maximum possible number of holes that do not suffer jet merging [23]. Whether it should be avoided depends on further details of the injection strategy. The jet merging, as mentioned before, is due to the Coanda effect, which in this case means the jets effectively entrain each other.

As a consequence of jet merging, at -130°CA the fuel is highly concentrated in a rich central core, which spreads as the jet travels downwards. The collapsed jets have penetrated all measurement planes, but it is not clear if they have impinged the piston and cylinder walls. As compression progresses the fuel that has been confined near the cylinder walls progressively makes its way back to the center of the cylinder, mixing with the bulk gas. In this mixing process, the tumble motion of the bulk gas slightly breaks the symmetry of the injector and cylinder geometry such that an elongated off-center lean region is formed. The final mixture appears relatively homogeneous, possibly helped by the squish flow, which promotes mixing just before "ignition".

The evolution for the intermediate injection timing with SOI = -80°CA shows a trend similar to the early-injection case. Jet merging with star-shaped contours, at planes close to the injector nozzle, is observed as well for this timing. At -55° CA, shortly after the injection has ended, a slight deflection of the jet wake can be seen. The deflection could be due to the action of the in-cylinder bulk flow on the jet that has lost momentum after the end of injection. Impingement of the jet on the piston top is observed very clearly in this case. Not much of the wall-jet structure can be discerned in the color map chosen here for consistency with other cases and times. As for previous multi-hole injectors, at -40°CA much of the fuel is not in the field of view because it is confined to near the cylinder walls. Again, for this intermediate-injection timing there is not enough time for these rich mixtures to convect to center of the chamber; in other words, the squish flow is not strong enough to push the near-wall fuel inwards. Consequently, at spark timing the center is very lean, probably too lean to be ignitable.

Injecting the fuel late (SOI = -40°CA) results in an earlier and stronger jet-piston interaction, simply due to the proximity of piston and injector. Figure 7 shows that by -30°CA the jet has impinged onto the top surface of the piston. A cross-section through the top of the recirculation vortex of the wall jet appears as an annular band that surrounds the jet core (bottom plane). As the piston moves towards TDC the fuel injection continues and the wall jet grows covering first the entire piston top-surface and then the cylinder walls. Again, due to the short time between injection and "ignition" the fuel from the recirculation zones does not convect back to the region near the spark-plug location. At the last image timing, the injection has left a small fuel-rich zone near the injector. It is not clear if in fired operation the extent of this rich area is consistently large enough to reliably provide an ignitable mixture. It appears that even this latest injection timing leaves the fuel unfavorably concentrated near the walls.

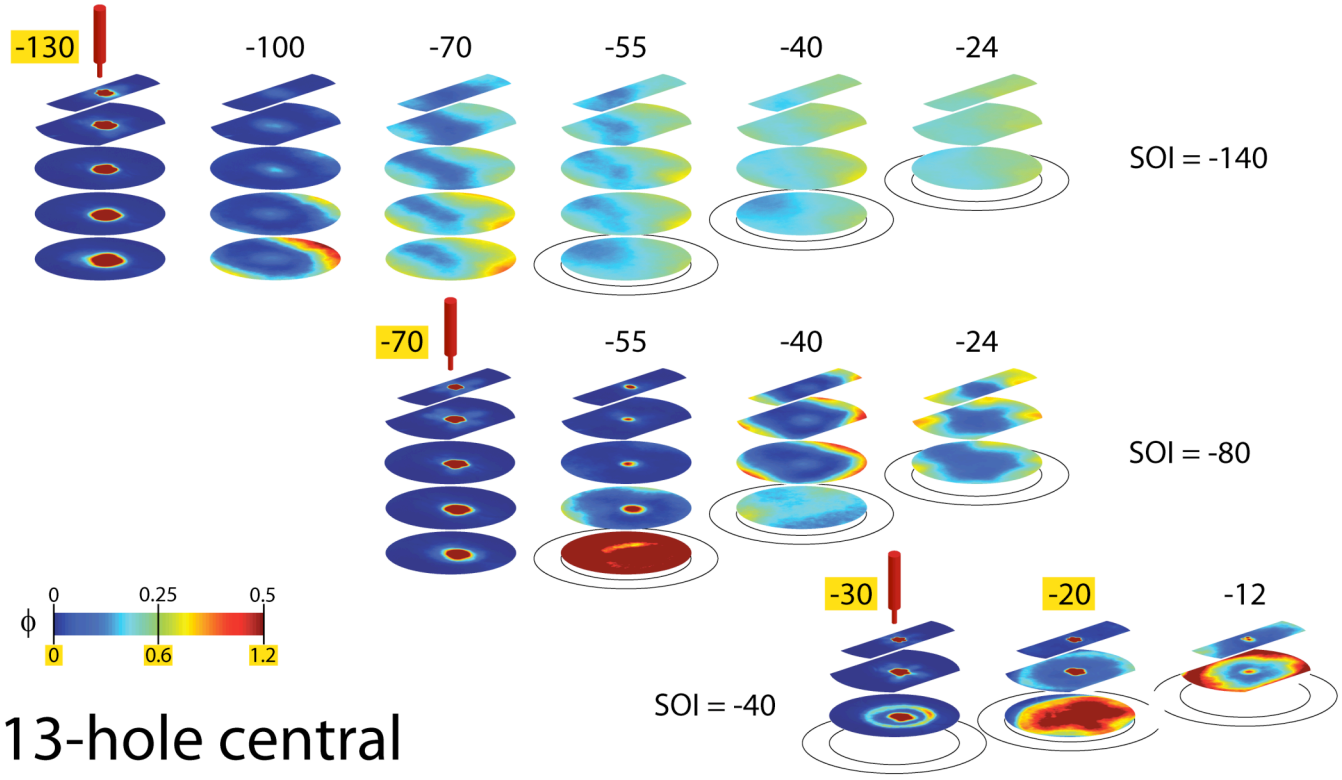

Figure 7: Same type of time series as in Figure 4 for the 13-hole injector in central position, *i.e.,* time series of the *mean* equivalence ratio from PLIF measurements.

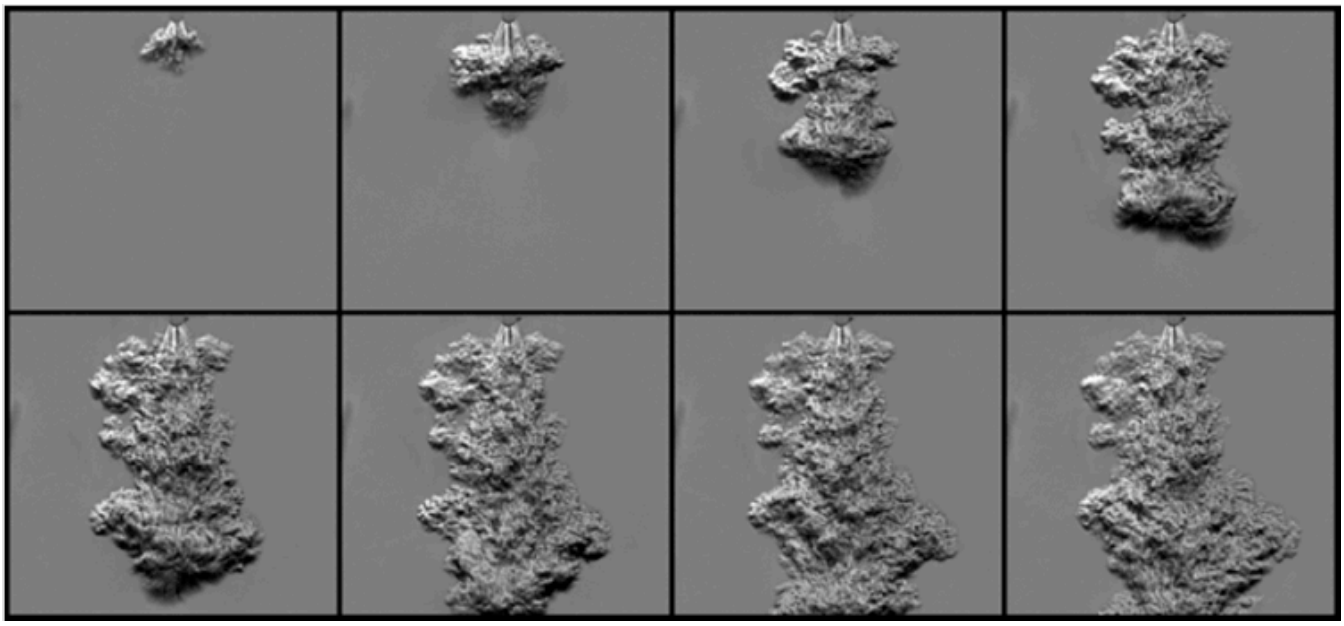

Figure 8: Time series of a *single* injection event (side view) from the 13-hole injector using a high-speed Schlieren system in a pressurized vessel with an ambient density of 3.4 kg/m^3. The time interval between images here is 122 μs. Each image corresponds to an area of 83 mm x 75 mm (width x height). Reproduced by permission of the author [22].

COMPARISON OF THE STRATIFICATION AT SOI = -80°CA

The intermediate injection timing, SOI = -80°CA, is an interesting case in that the fuel jets interact with the walls and themselves much more than for later injection, yet the final mixture is much more inhomogeneous than it is for earlier injection. Thus one would expect large differences in the final mixture stratification.

Figure 9 directly compares the fuel distributions at the time of "spark" for the different injector configurations. Since imaging in the squish volume is not possible at -16°CA, the image set for 5-hole down has been augmented by the up-most plane in the squish volume from -30°CA. Surprisingly, the fuel distribution for all six configurations is quite similar, except for the single-hole injector, where high levels of stratification and fuel confinement in only one side of the combustion chamber is seen. All multi-hole configurations feature a very lean zone in the center, with equivalence ratios of 0.1 and less, and conversely most of the fuel is concentrated towards the side walls of the combustion chamber, with peak equivalence ratios of 0.3 - 0.45. Also, in all configurations horizontal inhomogeneity dominates vertical stratification, *i.e.*, in each image set all planes are similar. From a practical point of view all six spatial distributions are unfavorable, since fuel is located next to the wall and would burn with high heat and crevice losses. Admittedly, no effort was made to optimize the piston-top surface to redirect the jets in a favorable way, as for example in many wall-guided GDI systems. Nevertheless, it can be seen that only for very late injection the fuel can be expected to actually be anywhere near the injector at the time of spark.

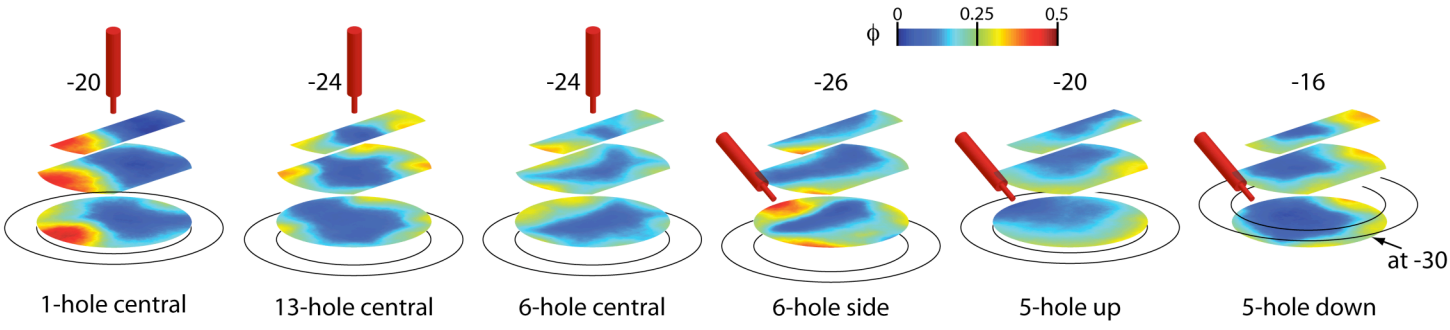

Figure 9: Mean equivalence ratio at MBT spark timing for SOI = -80°CA. Injector configuration and spark timing as indicated in figure. See text for comments on the bottom-most imaging plane for "5-hole down".

CONCLUSIONS

Planar Laser-Induced Fluorescence of acetone as a fuel tracer was applied in a motored hydrogen DI engine. The characteristics of six different injector geometries and configurations and three different injection timings were investigated. The evolution of the mixture from mid-injection to a presumed spark timing can be summarized as follows:

- For the single-hole injector, the jet momentum is spatially concentrated. The orientation of the nozzle at an angle with respect to the vertical results in extensive redirection of the jet by the walls, yielding a tumble-like circular motion within the cylinder.

- After end of injection, the volume just downstream of any injector becomes almost devoid of fuel, in qualitative agreement with the enhanced mixing [19] observed at the end of injection for diesel jets [18]. This process here takes about 20°CA, longer than in the diesel jets investigated in the references above. The vastly different ratio of the densities of air and fuel, or details of the injection ramp-down might be responsible for this difference from diesel jets.

- Fast jet penetration and long available time make jet-jet and jet-wall interactions the dominating mechanism in mixture preparation for early and intermediately timed injection. Higher pressure towards the end of the compression stroke slows fuel penetration significantly.

- As far as can be deduced without direct velocity measurements, intake-induced bulk-gas tumble has negligible influence on mixture formation with the single-hole injector, which is in a “cross-wind” configuration with respect to bulk-gas tumble. There is minor influence on charge motion for some of the multi-hole injectors.

- Individual jets collapse into a single central jet due to jet-to-jet merging for the 13-hole injector. This happens for all injection timings and is a consequence of the small angular spacing of the jets. Consequently, mixing is dominated by downstream jet-wall interaction with little near-field entrainment of the merged jet.

- Partial jet merging and large-scale turbulent fluctuations lead to near-field jet instabilities for the 5-hole injector, which has a central jet and a smaller cone angle than the 6-hole injector

- For SOI = -80°CA, the fuel distribution at the time of “spark” is surprisingly similar for all five multi-hole configurations, and it is unfavorable for all five. This distribution is a consequence of the downward jet momentum interacting with the piston top, spreading the jet into the squish zone, without sufficient time to re-emerge into the center of the combustion chamber.

ACKNOWLEDGEMENTS

The excellent technical support by G. Hux and K. St. Hillaire at Sandia is greatly appreciated, as are valuable contributions by Thomas Wallner’s group at Argonne National Laboratory. Benjamin Peterson provided the high-speed Schlieren images in Figure 8, taken at the University of Wisconsin. Financial support for this research was provided by the U.S. Department of Energy, Office of Energy Efficiency and Renewable Energy. The research was performed at the Combustion Research Facility, Sandia National Laboratories, Livermore, California. Sandia is operated by Sandia Corporation, a Lockheed Martin Company, for the United States Department of Energy’s National Nuclear Security Administration under contract DE-AC04-94AL85000. The authors wish to thank Gurpreet Singh, program manager at DOE, for his support.

REFERENCES

[1] Welch, A., Mumford, D., Munshi, S., Holbery, J., and Boyer, B., “Challenges in Developing Hydrogen Direct Injection Technology for Internal Combustion Engines,” SAE Paper 2008-01-2379, 2008.

[2] Eichlseder, H., Wallner, T., Freyman, R., and Ringler, J., “The Potential of Hydrogen Internal Combustion Engines in a Future Mobility Scenario,” SAE Paper 2003-01-2267, 2003.

[3] Rottengruber, H., Berckmüller, M., Elsässer, G., Brehm, N., and Schwarz, C., “Direct Injection Hydrogen SI Engine Operation Strategy and Power Density Potentials,” SAE Paper 2004-01-2927, 2004.

[4] White, C. M., Steeper, R. R., and Lutz, A. E., “The Hydrogen Fueled Internal Combustion Engine: A Technical Review,” Int. J. Hydrogen Energy 31: 1292-1305, 2006

[5] Wallner, T., Nande, A. M., and Naber, J., “Evaluation of Injector Location and Nozzle Design in a Direct-Injection Hydrogen Research Engine,” SAE Paper 2008-01-1785, 2008.

[6] White, C. M., “OH* Chemiluminescence Measurements in a Direct Injection Hydrogen-Fuelled Engine,” Int. J. Engine Research 8: 185-204, 2007.

[7] White, C. M., “A Qualitative Evaluation of Mixture Formation in a Direct-Injection Hydrogen-Fuelled Engine,” SAE Paper 2007-01-1467, 2007.

[8] Kaiser, S. A., and White, C. M., “PIV and PLIF to Evaluate Mixture Formation in a Direct-Injection Hydrogen-Fuelled Engine,” SAE Paper 2008-01-1034, 2008.

[9] Wallner, T., Nande, A. M., and Naber, J. D., “Study of Basic Injection Configurations using a Direct-Injection Hydrogen Research Engine,” SAE Paper 2009-01-1418, 2009

[10] Salazar, V. M., Kaiser, S. A., and Halter, F., “Optimizing Precision and Accuracy of Quantitative PLIF of Acetone as a Tracer for Hydrogen Fuel,” SAE Paper 2009-01-1534, 2009.

[11] Thurber M.C., Grisch F., Kirby B.J., Votsmeier M., and Hanson R.K., “Measurements and Modeling of Acetone Laser-Induced Fluorescence with Implications for Temperature-Imaging Diagnostics”, Appl. Opt. 37: 4963–78, 1998.

[12] Thurber M.C., and Hanson R.K., “Pressure and Composition Dependences of Acetone Laser-Induced Fluorescence with Excitation at 248, 266 and 308 nm”, Appl. Phys. B 69:229-240, 1999.

[13] Yeh C. N., Kamimoto T., Kosaka H., and Kobori S., “Quantitative Measurement of 2-D Fuel Vapor Concentration in a Transient Spray Via Laser-Induced Fluorescence Technique,” SAE Paper 941953, 1994

[14] Espey C., Dec J.E., Leitzinger T.A., and Santavicca D.A., “Planar Laser Rayleigh Scattering for Quantitative Vapor-Fuel Imaging in a Diesel Jet”, Comb. Flame 109: 65-89, 1997.

[15] Hwang, W., Dec J.E., and Sjöberg M., “Fuel Stratification for Low-Load HCCI Combustion: Performance & Fuel-PLIF Measurements”, SAE Paper 2007-01-4130, 2007.

[16] Kirchweger, W., Haslacher, R., Hallmannsegger, M., and Gerke, U., “Application of the LIF Method for the Diagnostics of the Combustion Process of Gas-IC-Engines,” Exp. Fluids 43: 329–340, 2007

[17] Johari, H., and Paduano, R., “Dilution and Mixing in an Unsteady Jet,” Exp. Fluids 23: 272-280, 1997.

[18] Genzale, C. L., Reitz, R. D., and Musculus, M. P. B., “Effects of Piston Bowl Geometry on Mixture Development and Late-Injection Low-Temperature Combustion in a Heavy-Duty Diesel Engine,” SAE Paper 2008-01-1330, 2008.

[19] Musculus, M. P. B., and Kattke, K., “Entrainment Waves in Diesel Jets,” SAE Paper 2009-01-1355, 2009.

[20] Naber, J.D., and Siebers, D.L. “Effects of gas density and vaporization on penetration and dispersion of diesel sprays,” SAE Paper 960034, 1996.

[21] Messner, U., Wimmer, A., Gerke, U., and Gerbig, F., “Application and Validation of the 3D CFD Method for a Hydrogen Fueled IC Engine with Internal Mixture Formation,” SAE Paper 2006-01-0448, 2006.

[22] Petersen, B. R., “Transient High-Pressure Hydrogen Jets Measurements,” M.S. Thesis, University of Wisconsin-Madison, 2006

[23] Jennigs, M.J., and Jeske, F.R., “Analysis of the Injection Process in Direct Injected Natural Gas Engines: Part II- Effects of Injector and Combustion Chamber Design”, *ASME J. Eng. for Gas Turbines and Power* 116: 806-813, 1994.

Author contact:

Sebastian Kaiser sakaise@sandia.gov

Sandia National Laboratories

P.O. Box 969, MS 9053

Livermore, CA 94551